The Journal of Immunology

RESEARCH ARTICLE | AUGUST 15 2021

Fractalkine Elicits Chemotactic, Phenotypic, and Functional Effects on CX3CR1^{+}CD27^{-} NK Cells in Obesity-Associated Cancer FREE

Eimear Mylod; ... et. al

J Immunol (2021) 207 (4): 1200–1210.
https://doi.org/10.4049/jimmunol.2000987

Fractalkine Elicits Chemotactic, Phenotypic, and Functional Effects on CX3CR1^{+}CD27^{-} NK Cells in Obesity-Associated Cancer

Eimear Mylod,* Ashanty M. Melo,*,[1] Noel E. Donlon,*,†,[1] Maria Davern,* Anshul Bhardwaj,‡ John V. Reynolds,† Joanne Lysaght,*,[2] and Melissa J. Conroy*,[2]

Esophagogastric adenocarcinomas (EAC) are obesity-associated malignancies underpinned by severe immune dysregulation and inflammation. Our previous work indicates that NK cells migrate to EAC omentum, where they undergo phenotypic and functional alterations and apoptosis. In this study, we investigate whether such erroneous chemotaxis to omentum is paralleled by compromised NK cell infiltration of EAC patient tumor and examine the role of the inflammatory chemokine fractalkine in shaping the NK cell–mediated response. Our data show diminished NK cell frequencies in EAC tumor compared with those in the circulation and reveal that intratumoral NK cell frequencies decline as visceral obesity increases in EAC patients. Our in vitro findings demonstrate that antagonism of fractalkine receptor CX3CR1 significantly reduces NK cell migration to EAC patient–derived, omental adipose tissue–conditioned media, but not toward tumor-conditioned media. These data suggest fractalkine is a key driver of NK cell chemotaxis to omentum but has a lesser role in NK cell homing to tumor in EAC. We propose that this may offer a novel therapeutic strategy to limit NK cell depletion in the omentum of obese EAC patients, and our data suggest the optimal timing for CX3CR1 antagonism is after neoadjuvant chemoradiotherapy. Our functional studies demonstrate that fractalkine induces the conversion from CX3CR1^{+}CD27^{-} to CX3CR1^{-}CD27^{+} NK cells and increases their IFN-γ and TNF-α production, indicative of its role in shaping the dominant NK cell phenotype in EAC omentum. This study uncovers crucial and potentially druggable pathways underpinning NK cell dysfunction in obesity-associated cancer and provides compelling insights into fractalkine's diverse biological functions. ***The Journal of Immunology*****, 2021, 207: 1200–1210.**

The global obesity epidemic, now termed "globesity," continues to contribute to the increased prevalence of noncommunicable disease, such as diabetes and cancer (1). Esophageal, gastric, and gastroesophageal junctional adenocarcinomas fall under the umbrella of esophagogastric adenocarcinomas (EAC), a group of obesity-associated and inflammation-driven malignancies (2, 3). The dismal five-year survival rates for esophageal adenocarcinoma and gastric adenocarcinoma of 20 and 32%, respectively, are largely due to poor treatment response rates of <30% (4–8).

NK cells are innate effector lymphocytes with potent cytokine-producing and cytotoxic capabilities and play a key role in tumor immunosurveillance (9, 10). Our group has previously reported active recruitment of immune cells, including NK cells, to the soluble chemotactic cues from visceral adipose tissue (VAT), namely the omentum in EAC patients (11, 12). Furthermore, we have shown that soluble factors in EAC omentum induce NK cell functional changes and apoptosis, thus reducing their potential to elicit effective antitumor immunity (12). Consequentially, low infiltrations of NK cells have been reported in esophageal and gastric tumors and are associated with a poorer prognosis in these patients (13, 14). Alterations in NK cell frequency and attenuation of their effector function are well documented in obesity and obesity-associated cancer (12, 15–21). We propose that diminished NK cell frequency and function contributes to extensive immune dysregulation and compromised antitumor immunity in EAC. Therefore, such patients are likely to benefit from immunotherapeutic approaches that can halt the erroneous migration of NK cells to the omentum while restoring their numbers and promoting their infiltration of tumor.

The multifaceted functionality of chemokines as regulators of cell migration and mediators of inflammation has piqued an interest in their immunotherapeutic potential (22). In obesity, a loss of adipose tissue homeostasis is coupled with dysregulated chemokine production and release from the omentum, leading to the recruitment of inflammatory immune cells, which rapidly accumulate and contribute to obesity-associated inflammation (23).

A role for the inflammatory chemokine fractalkine (CX3CL1) in macrophage-mediated inflammation in adipose tissue has been established in obesity (24). In EAC, our group has shown that T cells are recruited to the omentum by proinflammatory chemokines, where

*Cancer Immunology and Immunotherapy Group, Department of Surgery, Trinity Translational Medicine Institute and the Trinity St. James's Cancer Institute, St. James's Hospital, Trinity College Dublin, Dublin, Ireland; †Gastro-intestinal Medicine and Surgery, St. James's Hospital, Dublin, Ireland; and ‡Department of Surgery, Trinity College Dublin and St. James's Hospital, Dublin, Ireland

[1]A.M.M. and N.E.D. contributed equally to this work.

[2]J.L. and M.J.C. are cosenior authors.

ORCIDs: 0000-0002-7324-1732 (E.M.); 0000-0002-4073-3896 (N.E.D.); 0000-0003-2278-5497 (M.D.); 0000-0003-4421-8987 (A.B.); 0000-0003-3363-3763 (J.L.); 0000-0002-3822-0442 (M.J.C.).

Received for publication August 26, 2020. Accepted for publication May 30, 2021.

This work was supported by Breakthrough Cancer Research Grant BCR-2019-02-PhD-TCD, Irish Research Council Award GOIPD/2015/272, and M.Sc. in Molecular Medicine in Trinity College Dublin.

Address correspondence and reprint requests to Dr. Melissa J. Conroy, Cancer Immunology and Immunotherapy Group, Trinity Translational Medicine Institute and the Trinity St. James's Cancer Institute, Department of Surgery, Trinity College Dublin, St. James's Hospital, Dublin 8, Ireland. E-mail address: meconroy@tcd.ie.

Abbreviations used in this article: ACM, adipose tissue–conditioned medium; BMI, body mass index; CRT, chemoradiotherapy; EAC, esophagogastric adenocarcinoma; TCM, tumor tissue–conditioned medium; VAT, visceral adipose tissue; VFA, visceral fat area;

www.jimmunol.org/cgi/doi/10.4049/jimmunol.2000987

they contribute to pathological obesity-associated inflammation (11, 25, 26). Importantly, we have identified that fractalkine governs cytotoxic $CD8^+$ T cell migration to omentum in EAC and mediates subsequent phenotypic alterations to these potent antitumor cells, potentially at the expense of effective cytotoxic T cell–mediated antitumor immunity (11). In this study, we have examined the role of fractalkine as a modulator of NK cell migration and phenotype to explore whether this pathway can be exploited with therapeutic intent to boost NK cell infiltration of EAC tumors.

We report that NK cell frequencies are diminished in both EAC tumor and omentum, compared with the blood, with lowest intratumoral frequencies observed in the most viscerally obese patients. Furthermore, NK cell migration toward chemotactic cues in EAC omentum, but not tumor, can be significantly reduced by antagonizing the fractalkine receptor CX3CR1. Importantly, this approach could be used to increase the availability of NK cells for migration toward alternative chemotactic signals in EAC tumor (27). In addition, we have identified that fractalkine induces a conversion from $CX3CR1^+CD27^-$ to a $CX3CR1^-CD27^+$ phenotype in NK cells, which is representative of the dominant NK cell phenotype in EAC omentum and is well established as the less cytolytic and predominantly cytokine-producing population (28–30). Interestingly, our data demonstrate that fractalkine also increases IFN-γ and TNF-α production by NK cells, indicative of its role in shaping their functional profile and reaffirming its important role as a regulator of cytotoxic lymphocyte function. We propose that fractalkine is a key regulator of NK cells in EAC and suggest that CX3CR1 antagonism has potential to overcome a key challenge in obesity-associated cancer by preventing NK cell trafficking to omentum and limiting their dysfunction in viscerally obese EAC patients.

Materials and Methods

Patient demographics

A total of 71 patients attending the National Esophageal and Gastric Centre at St. James's Hospital, Dublin, Ireland, were enrolled in this study from 2017 to 2020. Treatment-naive blood and tumor tissues were collected from 15 patients. Blood, omentum, and tumor tissues were collected from 60 patients following neoadjuvant chemoradiotherapy (CRT) at time of surgical resection. Body mass index (BMI), visceral fat area (VFA), and anthropometric variables were measured, as described previously (Table I) (31, 32). The group consisted of 55 males and 16 females, representative of the predominance of EAC in males, with an average age of 63.5 y. The mean BMI at the time of surgery was 29.7 kg/m^2, making 77% overweight or obese, and the mean VFA by computed tomography scan was 127.8 cm^2. Neoadjuvant CRT was administered to 73% of patients.

The work was performed in accordance with the Code of Ethics of the World Medical Association (Declaration of Helsinki) for experiments involving humans. Patients provided informed consent for sample and data acquisition, and the study received full ethical approval from the St. James's Hospital Ethics Review Board. Patient samples were pseudonymized to protect the privacy rights of the patients.

Sample preparation

Blood, omental adipose tissue samples, and tumor biopsies were collected during surgical resection. PBMC were prepared by density gradient centrifugation. Omental adipose tissue samples (5 g) were enzymatically digested with collagenase type II to obtain the stromal vascular fraction as previously described with a shorter collagenase treatment time of 20 min, optimized to prevent the loss of NK cell surface receptor expression (12, 32). Tumor biopsies were enzymatically digested with collagenase type IV as previously described with a shorter collagenase treatment time of 20 min (33). Adipose tissue–conditioned media (ACM) was prepared as previously described (32), and tumor tissue–conditioned media (TCM) was prepared by culturing the tumor biopsy in 1 ml of M199 medium supplemented with 1% gentamicin at 37°C, 5% CO_2 for 24 h.

Quantification of $CX3CR1^+$ NK cells in EAC blood, omentum, and tumor

Treatment-naive and posttreatment whole-blood and intratumoral immune cells and posttreatment stromal vascular fraction from omentum were stained with CD56-FITC-VioBright, CD3-PE-Cy7, CX3CR1-PE, CD27-PE-VioGreen (Miltenyi Biotec), ICAM-1–allophycocyanin, L-selectin–BV510, CD3-PerCp-Cy5.5, CD27-AmCyan, CX3CR1-BV650 (BioLegend), CD3-PE–eFluor 610, L-selectin–AF700 (BD Biosciences), and CD27-allophycocyanin–eFluor 780 (eBioscience). Staining with annexin V–FITC, CD3-allophycocyanin-Cy7 (BioLegend), and CD56-allophycocyanin (Miltenyi Biotec) was carried out to detect apoptotic NK cells. RBCs were lysed using BD Lysing Solution (BD Biosciences) as per the manufacturer's instructions. NK cells were quantified as $CD56^+CD3^-$ cells within the lymphocyte gate. $CX3CR1^+$ NK cells were quantified as a proportion of $CD56^+CD3^-$ lymphocytes. Cells were acquired using the CyAn ADP (Beckman Coulter), CANTO II (BD Biosciences), or LSR Fortessa (BD Biosciences) flow cytometer and analyzed using FlowJo software (Tree Star).

Table I. Patient demographic table

Age (y)	63.5
Sex ratio (M/F)	55:16
Diagnosis (no. of patients)	
EAC	39
EGJ	12
Gastric	20
Tumor stage[a] (no. of patients)	
T0	7
T1	16
T2	9
T3	22
T4	9
Nodal status[b] (no. of patients)	
Positive	27
Negative	30
Mean BMI (kg/m^2)[c]	29.7
BMI (no. of patients)	
Underweight (BMI <19.9)	1
Normal weight (BMI 20–24.9)	13
Overweight (BMI 25–29.9)	27
Obese (BMI >30)	22
Mean VFA (cm^2)	127.8
Viscerally obese by VFA[d]	40.9%
Received neoadjuvant CRT[e]	73%

[a]Tumor staging could not be determined for eight patients.
[b]Nodal status could not be determined for 14 patients.
[c]BMI could not be determined for eight patients.
[d]Obese VFA >160 cm^2 for men and >80 cm^2 for women (31). Calculated for a total of 66 patients.
[e]Of the patients, 4.2% received chemotherapy only.
EGJ, gastroesophageal junctional adenocarcinoma; F, female; M, male.

NK cell chemotaxis assays

PBMC were isolated from noncancer blood by density gradient centrifugation, resuspended in RPMI 1640 medium, and treated with 80 μM of CX3CR1 antagonist AZD8798 (Axon MedChem) for 1 h. Cells were subsequently added at a density of 0.2×10^6 cells/100 μl RPMI 1640 medium to a 5-μm pore Transwell filter system (Corning) with ACM or TCM added in the lower chamber. M199 alone was used as a negative control, and M199 supplemented with 20% FBS was used as a positive control. This system was incubated for 2 h at 37°C, 5% CO_2. Cells were collected from the lower chamber and stained for flow cytometric analysis with CD56-FITC-VioBright and CD3-PE-Cy7 (Miltenyi Biotec). CountBright beads (Thermo Fisher Scientific) were used to enumerate the migrated $CD56^+CD3^-$ NK cells. Cells were acquired using the CyAn ADP (Beckman Coulter) flow cytometer and analyzed using FlowJo software (Tree Star).

CX3CR1 surface expression by NK cells following recombinant fractalkine treatment

PBMC were isolated from noncancer controls by density gradient centrifugation and seeded at a density of 1×10^6 cells/ml RPMI 1640 medium supplemented with 10% FBS and 1% penicillin–streptomycin. Cells were treated with 30 ng/ml recombinant fractalkine (BioLegend), which is the mean concentration of fractalkine in EAC omentum, for 2 or 24 h. Cells were stained with CD56-FITC-VioBright, CX3CR1-PE (Miltenyi Biotec), L-selectin–BV510, ICAM-1–allophycocyanin, CD3-allophycocyanin-Cy7, and CD27-BV510 (BioLegend) and acquired using the CANTO II (BD Biosciences) flow cytometer and analyzed using FlowJo software (Tree Star).

Cytokine profiling of NK cell following recombinant fractalkine treatment

PBMC were isolated from noncancer controls by density gradient centrifugation and seeded at a density of 1×10^6 cells/ml RPMI 1640 medium supplemented with 10% FBS and 1% penicillin–streptomycin. Cells were treated with 30 ng/ml recombinant fractalkine (BioLegend) for 2 or 24 h. Cells were subsequently stimulated with 30 ng/ml IL-12 and 100 ng/ml IL-15 (ImmunoTools) for a total of 18 h. After 15 h of stimulation, 10 μg/ml brefeldin A (Sigma-Aldrich) was added. Surface staining for CD56-FITC-VioBright, CX3CR1-PE (Miltenyi Biotech), and CD3-allophycocyanin-Cy7 (BioLegend) was performed. Subsequent intracellular staining for TNF-α–allophycocyanin, IL-10–BV421, and IFN-γ–BV510 (BioLegend) was performed using FIX&PERM Cell Fixation and Permeabilization Kit (Nordic-MUBio). Cells were acquired using the CANTO II (BD Biosciences) flow cytometer and analyzed using FlowJo software (Tree Star).

NK cell degranulation assay

PBMC were isolated from noncancer controls by density gradient centrifugation and seeded at a density of 1×10^6 cells/ml RPMI 1640 medium supplemented with 10% FBS and 1% penicillin–streptomycin. Cells were treated with 30 ng/ml recombinant fractalkine (BioLegend) for 2 or 24 h. Cells were subsequently stimulated with 30 ng/ml IL-12 and 100 ng/ml IL-15 (ImmunoTools) for a total of 18 h. After 14 h of stimulation, CD107a-PE-Cy7 (BioLegend) was added for 1 h, followed by addition of 10 μg/ml brefeldin A (Sigma-Aldrich) for the remaining 3 h. Surface staining for CD56-FITC-VioBright, CX3CR1-PE (Miltenyi Biotech), and CD3-allophycocyanin-Cy7 (BioLegend) was performed. Cells were acquired using the CANTO II (BD Biosciences) flow cytometer and analyzed using FlowJo software (Tree Star).

NK cell cytotoxicity assay

Noncancer control primary NK cells were isolated from PBMC by magnetic cell sorting using human NK cell isolation kit (STEMCELL Technologies) according to the manufacturer's instructions. NK cells were treated with 30 ng/ml recombinant fractalkine (BioLegend) and stimulated with 100 IU IL-2 (PeproTech) for 24 h. NK cell cytotoxicity was quantified with the Cell-Mediated Cytotoxicity Assay (ImmunoChemistry Technologies). Briefly, K562 target cells were stained with CFSE. NK cells were cocultured with stained K562 cells for 4 h. SR-FLICA and 7-aminoactinomycin D were used to quantify apoptotic and dead cells, respectively. Cells were acquired using the CANTO II (BD Biosciences) flow cytometer and analyzed using FlowJo software (Tree Star).

Statistical analysis

Statistical analysis was carried out using GraphPad Prism, version 8 (GraphPad Software). Differences between groups were analyzed using one-way ANOVA with Bonferroni post hoc test or paired *t* test when appropriate. A p value <0.05 was considered significant.

Results

Significantly lower frequencies of NK cells in the omentum and tumor compared with those in the blood of EAC patients

To ascertain the distribution of NK cells, the frequencies of $CD56^+CD3^-$ cells were quantified as a percentage of the total lymphocyte population in the blood ($n = 21$), omentum ($n = 25$), and tumor ($n = 11$) of EAC patients (Fig. 1). Our data identified significantly lower frequencies of NK cells in EAC omentum and tumor compared with those in the blood: blood versus omentum (7.89 versus 4.13%, $p = 0.0252$) and blood versus tumor (7.89 versus 2.1%, $p = 0.0046$) (Fig. 1A). Whereas intratumoral NK cell frequencies were the lowest of all compartments examined, there were no significant differences between NK cell frequencies in the omentum and tumor of EAC patients: omentum versus tumor (4.13 versus 2.1%, $p = 0.7147$) (Fig. 1A).

We next sought to determine the association between obesity and the frequency of NK cells in the tumor of EAC patients. There was a significant negative correlation between VFA and total NK cell frequency within the tumor of EAC patients ($r = -0.73$, $p = 0.03$, $n = 9$) (Fig. 1C). This suggests that frequencies of intratumoral NK cells decrease as visceral obesity increases in EAC. Interestingly, when

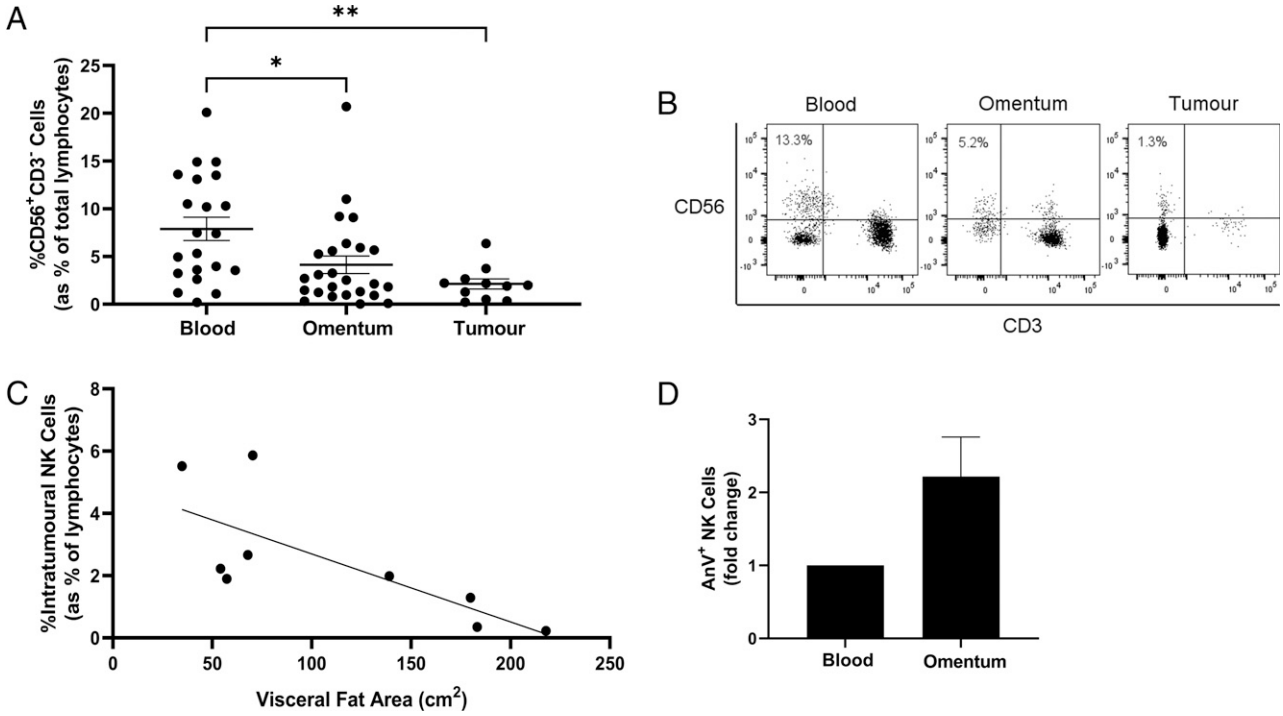

FIGURE 1. Significantly lower frequencies of NK cells in the omentum and tumor of EAC patients compared with those in blood. (**A**) Scatterplot showing the frequencies of $CD56^+CD3^-$ (NK) cells as a percentage of total lymphocytes in the blood ($n = 21$), omentum ($n = 25$), and tumor ($n = 11$) of EAC patients. (**B**) Representative dot plots of NK cells ($CD56^+CD3^-$ lymphocytes) in blood, omentum, and tumor of EAC patients. (**C**) Line graph showing inverse correlation between VFA and the frequencies of intratumoral NK cells as a percentage of total lymphocytes in nine EAC patients. (**D**) Bar chart showing the fold change frequency of annexin V^+ (AnV^+) NK cells in the circulation and omentum of EAC patients. Mean ± SEM. $*p < 0.05$, $**p < 0.01$ by one-way ANOVA or paired *t* test.

correlated with BMI, the association between obesity status and NK cell frequency in the tumor was not observed (data not shown).

To determine the extent of NK cell apoptosis within the omentum of EAC patients, the frequencies of annexin V^+ NK cells were quantified in fresh samples of EAC patient blood and omentum. The frequencies of apoptotic NK cells within EAC omentum were substantially higher than within the circulation, supporting our hypothesis of the VAT as a tissue microenvironment that is more conducive to NK cell apoptosis (Fig. 1D).

CX3CR1 antagonism significantly reduces NK cell migration to chemotactic signals in EAC omentum, but not tumor

Our group have previously reported that NK cells are actively recruited to chemotactic cues in the omentum of EAC patients (12). In this article, we propose that targeting NK cell migration to EAC omentum may prevent their depletion in this compartment and serve to restore cytotoxic NK cell frequencies, ultimately augmenting antitumor immunity in EAC patients. Because EAC omentum is a fractalkine-rich environment, we hypothesized that targeting this chemokine pathway using an antagonist against the fractalkine receptor CX3CR1 would reduce NK cell migration (11).

To assess this in vitro, NK cell migration toward ACM, generated from the omentum of EAC patients, was measured following treatment with 80 μM of the CX3CR1 antagonist AZD8798 ($n = 6$) (Fig. 2A). M199 was used as a negative control, whereas M199 supplemented with 20% FBS was used as a positive control. NK cell migration toward the positive control was significantly higher compared with the negative control, demonstrating the functionality of our chemotaxis model: M199 versus M199 + FBS (1 versus 6.332, $p = 0.0204$) (Fig. 2A) and M199 versus M199 + FBS (1 versus 3.495, $p = 0.0344$) (Fig. 2B). Furthermore, migration toward ACM was significantly higher compared with M199 negative control: M199 versus ACM (1 versus 2.205, $p = 0.0271$).

Following treatment with AZD8798, the fold change in NK cell chemotaxis toward ACM was significantly reduced compared with NK cells treated with vehicle control alone: ACM versus AZD8798 (2.205 versus 1.182, $p = 0.0055$) (Fig. 2A). To ensure that CX3CR1 antagonism would not compromise crucial NK cell migration toward the chemotactic cues of the tumor, NK cell migration toward EAC TCM was also measured following treatment with AZD879. CX3CR1 antagonism had no significant effect on NK cell migration toward TCM: TCM versus AZD8798 (1.466 versus 1.011, $p = 0.5861$) (Fig. 2B).

Significantly lower frequencies of $CX3CR1^+$ NK cells in the omentum and tumor compared with those in the blood of EAC patients

To confirm that EAC patient–derived NK cells express the target of AZD8798, CX3CR1 surface expression by NK cells was quantified in EAC patient–derived blood ($n = 27$), omentum ($n = 33$), and tumor ($n = 7$). There were significantly higher frequencies of $CX3CR1^+$ NK cells in the blood of EAC patients compared with the omentum and tumor: blood versus omentum (76.3 versus 29.7%, $p < 0.0001$) and blood versus tumor (76.3 versus 8.89%, $p < 0.0001$) (Fig. 3A). There were no significant differences between $CX3CR1^+$ NK cell frequencies in the omentum and tumor of EAC patients (29.7 versus 8.89%, $p = 0.1016$) (Fig. 3A).

Fractalkine mediates changes in CX3CR1 surface expression on NK cells

We have previously reported that high levels of fractalkine in the omentum of EAC patients can induce endocytosis of CX3CR1 by $CD8^+$ T cells, leading to lower frequencies of omental $CD8^+$ T cells expressing the surface receptor (11). We have also shown that such internalization is exclusive to T cells expressing high levels of the receptor, whereas $CD4^+$ T cells were not susceptible to the effects of fractalkine (11). In this study, we hypothesized that the fractalkine-rich omentum similarly recruits NK cells with high CX3CR1 expression from the circulation and subsequently induces a reduction in their CX3CR1 surface expression.

To demonstrate this, peripheral blood NK cells from noncancer donors were treated with 30 ng/ml recombinant fractalkine for 2 or 24 h to simulate the physiological levels of fractalkine in EAC omentum (Fig. 4) (11). A significant reduction in the frequency of $CX3CR1^+$ NK cells was observed following 2- and 24-h treatments with fractalkine, compared with that in untreated controls ($n = 3$): untreated versus 2 h (89.73 versus 6.24%, $p = 0.0108$) and untreated versus 24 h (89.73 versus 2.1%, $p = 0.0271$) (Fig. 4A).

Fractalkine increases CD27 surface expression by NK cells

Fractalkine is diverse in function and biological effects, from a mediator of inflammation to a promoter of tumor cell metastasis (24, 34). Therefore, before therapeutically targeting this pathway, it is important to examine the biological effects of this chemokine in the context of NK cells in inflammation-driven cancer. We have previously reported that fractalkine increases L-selectin expression on $CD8^+$ T cells, and this may have effects on their lymph node

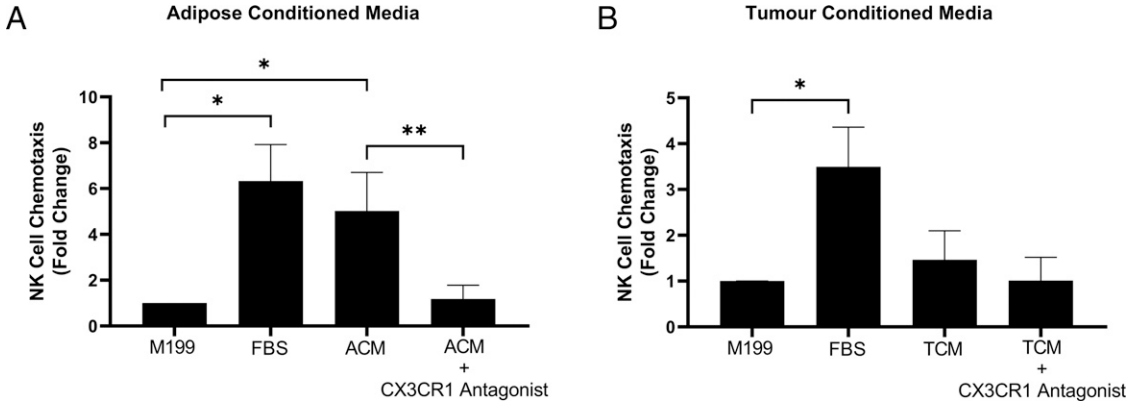

FIGURE 2. CX3CR1 antagonism significantly reduces NK cell chemotaxis to secreted factors from EAC omentum. (**A**) Bar charts showing the fold change migration of NK cells to M199 negative control ($n = 10$), M199 + FBS positive control ($n = 6$), and pretreated with vehicle control DMSO ($n = 10$) or 80 μM of CX3CR1 antagonist AZD8798 ($n = 6$) to EAC patient–derived ACM. (**B**) Bar charts showing the fold change migration of NK cells to M199 negative control ($n = 6$), M199 + FBS positive control ($n = 3$), and pretreated with vehicle control DMSO ($n = 6$) or 80 μM of CX3CR1 antagonist AZD8798 to EAC patient–derived tumor TCM ($n = 3$). Mean + SEM. $*p < 0.05$, $**p < 0.01$ by paired t test.

homing capabilities in EAC, with ramifications for their antitumor capabilities (11). To determine whether fractalkine mediates phenotypic alterations in NK cells, peripheral blood–derived NK cells were treated with 30 ng/ml recombinant fractalkine for 2 or 24 h ($n = 3$), and percentage frequencies of $CD27^+$, L-selectin$^+$, and ICAM-1^+ NK cells were quantified (Fig. 5). Following 24 h of culture in fractalkine, significantly higher proportions of $CD27^+$ NK cells were observed: untreated versus 24 h (2.64 versus 6.17%, $p = 0.0061$) (Fig. 5A, 5B). We next examined whether these significant changes mirrored the CD27 expression levels of NK cells in the fractalkine-rich environment of omentum in a total of 13 EAC patients. Indeed, there are significantly more $CD27^+$ NK cells in EAC omentum compared with the circulation or compared with tumor: omentum versus blood (40.93 versus 2.83%, $p = 0.0037$) and omentum versus tumor (40.93 versus 3.35%, $p = 0.0105$) (Fig. 5C). Analysis of coexpression of CX3CR1 and CD27 within our cohort reveals that most NK cells in the circulation are $CX3CR1^+CD27^-$, which have been established as the most mature and cytotoxic NK cell subset (Fig. 5D) (28, 30, 35). Moreover, our data reveal that there are significantly more $CX3CR1^+CD27^-$ in the circulation of EAC patients, compared with omentum and tumor: blood versus omentum (82.4 versus 22.9% $p < 0.0001$) and blood versus tumor (82.4 versus 12.2%, $p < 0.0001$) (Fig. 5D).

Unlike $CD8^+$ T cells, fractalkine treatment did not alter L-selectin or ICAM-1 surface expression by NK cells (Fig. 5A, 5B) (11). Frequencies of NK cells expressing the cell adhesion molecule L-selectin are significantly higher in the circulation, compared with the tumor: blood versus tumor (32.22 versus 6.49%, $p = 0.0179$) (Fig. 5C). Profiling of CX3CR1 and L-selectin coexpression in our cohort suggest circulating NK cells are predominantly CX3CR1$^+$ (Fig. 3A), with a proportion coexpressing both CX3CR1 and L-selectin, indicative of an effector population of NK cells (Fig. 5E) (36–38).

Fractalkine significantly increases the production of IFN-γ and TNF-α by NK cells

As fractalkine induces a conversion from a $CX3CR1^+CD27^-$ to a $CX3CR1^-CD27^+$ phenotype in NK cells, the effects of recombinant fractalkine treatment on IFN-γ, TNF-α, and IL-10 production were examined after 2 and 24 h ($n = 6$). To demonstrate that fractalkine induces the conversion in NK cell phenotype, the CX3CR1 and CD27 surface expression were first examined. There were significantly lower frequencies of CX3CR1$^+$ NK cells following treatment with fractalkine: untreated versus 24 h (85.5 versus 34.45%, $p = 0.0021$) (Fig. 6A). Similarly, there were significantly higher frequencies of $CD27^+$ NK cells following treatment with fractalkine: untreated versus 24 h (5.34 versus 9.03%, $p = 0.0174$) (Fig. 6B). Following 24 h of treatment with fractalkine, significantly higher proportions of NK cells producing the proinflammatory cytokines IFN-γ and TNF-α were observed: untreated versus 24 h (IFN-γ: 19.27 versus 42.77%, $p = 0.0479$; TNF-α: 28.05 versus 39.75%, $p = 0.0253$) (Fig. 6C, 6D). This suggests a role for fractalkine in shaping not only the phenotype of NK cells but also their functional profile.

Fractalkine does not alter the cytotoxic effector function of NK cells

To ascertain whether the changes reported in CD27 expression translated into alterations in the cytotoxicity of NK cells, their degranulation potential was assessed, and their cytotoxicity was quantified using K562 cells following treatment with fractalkine for 24 h. Fractalkine-mediated decreases in CX3CR1 and increases in CD27 surface expression were first confirmed. There were no significant differences in the frequencies of cells expressing the degranulation marker CD107a following 2 and 24 h of treatment with fractalkine ($n = 6$)

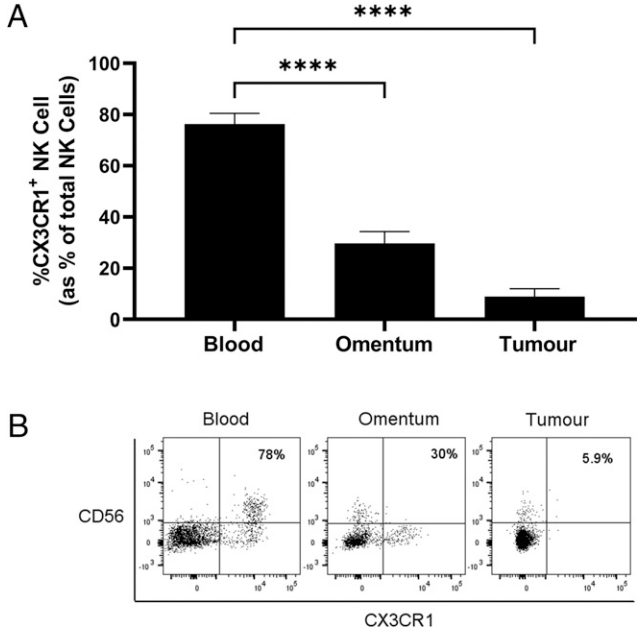

FIGURE 3. Significantly lower frequencies of CX3CR1$^+$ NK cells in the omentum and tumor of EAC patients compared with those in blood. (**A**) Bar chart showing the frequencies of CX3CR1$^+$ NK cells as a percentage of total NK cells in the blood ($n = 27$), omentum ($n = 33$), and tumor ($n = 7$) of EAC patients. (**B**) Representative dot plots showing gating of CX3CR1$^+$ NK cells previously gated on the total lymphocyte population in the blood, omentum, and tumor of EAC patients. Percentage frequencies shown are those of CX3CR1$^+$ NK cells as percentage of total NK cells. Mean + SEM. ****$p < 0.0001$ by one-way ANOVA.

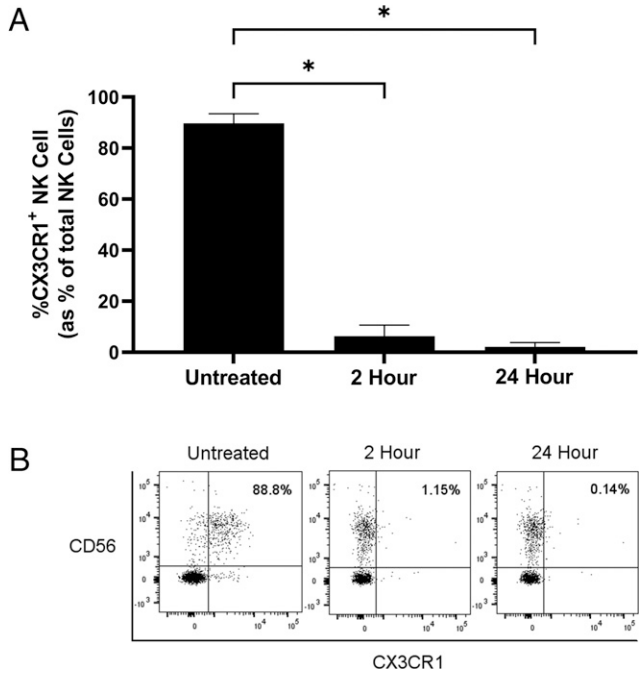

FIGURE 4. Fractalkine significantly reduces CX3CR1 surface expression by NK cells. (**A**) Bar chart showing the frequencies of CX3CR1$^+$ NK cells as a percentage of total NK cells following no treatment (Untreated) or treatment with 30 ng/ml recombinant fractalkine for 2 or 24 h ($n = 3$). (**B**) Representative dot plots showing peripheral blood–derived CX3CR1$^+$ NK cells previously gated on total lymphocytes following Untreated or treatment with 30 ng/ml recombinant fractalkine for 2 or 24 h. Percentage frequencies shown are those of CX3CR1$^+$ NK cells as percentage of total NK cells. Mean + SEM. *$p < 0.05$ by one-way ANOVA.

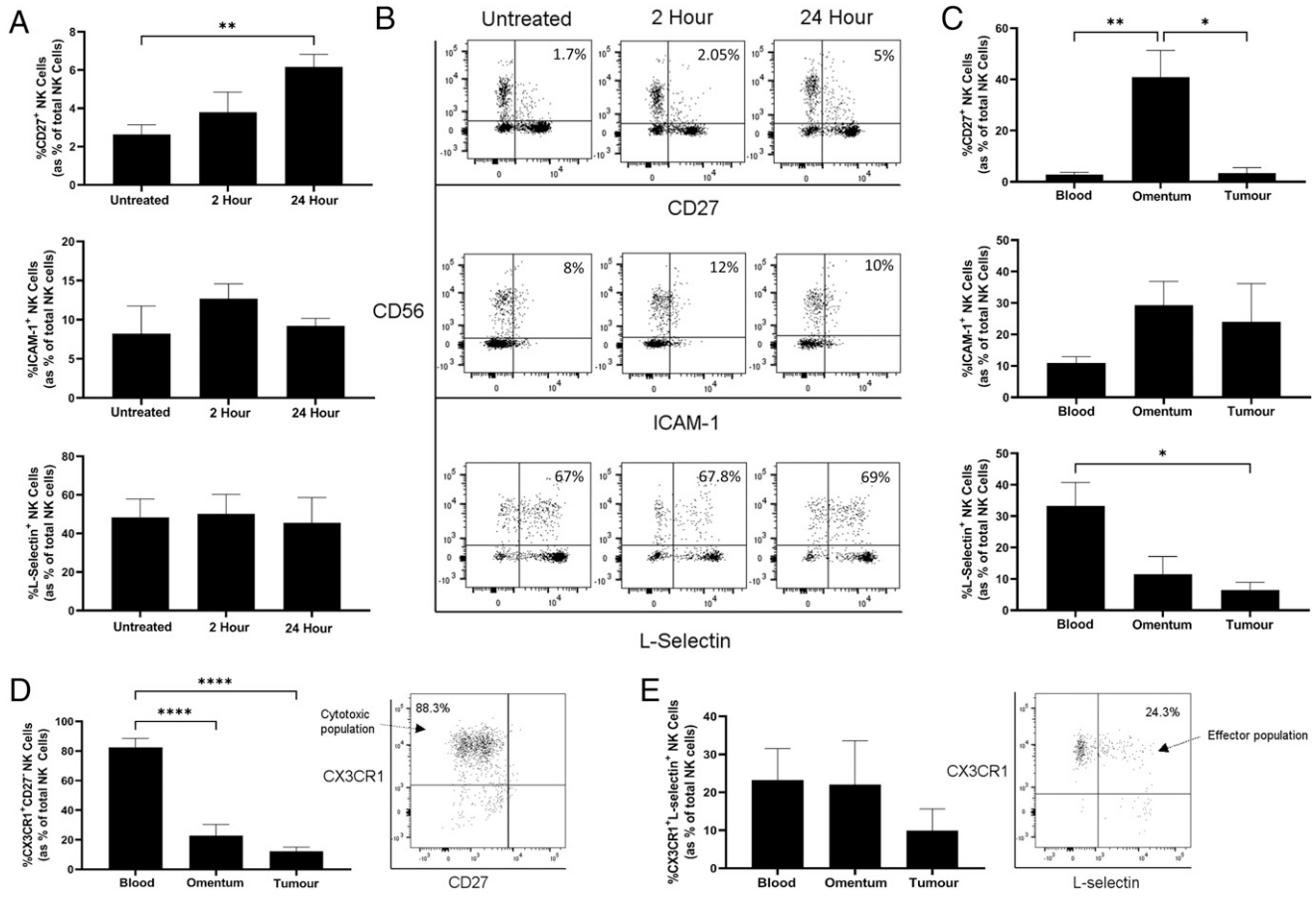

FIGURE 5. Significantly higher CD27 expression on NK cells following treatment with recombinant fractalkine and in the fractalkine-rich environment of omentum in EAC patients. (**A**) Bar chart showing the frequencies of $CD27^+$ (top), $ICAM\text{-}1^+$ (middle), and L-$selectin^+$ NK cells (bottom) as a percentage of total NK cells in healthy donor–derived PBMC following no treatment (Untreated) or following treatment with 30 ng/ml fractalkine for 2 or 24 h ($n = 3$). (**B**) Representative dot plots showing $CD27^+$ (top), $ICAM\text{-}1^+$ (middle), and L-$selectin^+$ NK cells (bottom) previously gated on total lymphocytes in healthy donor–derived PBMC following Untreated or following treatment with 30 ng/ml fractalkine for 2 or 24 h. Percentage frequencies shown on dot plots are those of $CD27^+$, $ICAM\text{-}1^+$, and L-$selectin^+$ NK cells as percentage of total NK cells, respectively. (**C**) Bar chart showing the frequencies of $CD27^+$ (top), $ICAM\text{-}1^+$ (middle), and L-$selectin^+$ NK cells (bottom) as a percentage of total NK cells in the blood, omentum, and tumor of EAC patients. CD27: blood $n = 10$, omentum $n = 13$, tumor $n = 7$. ICAM-1: blood $n = 4$, omentum $n = 5$, tumor $n = 4$. L-selectin: blood $n = 8$, omentum $n = 5$, tumor $n = 6$. (**D**) Left, Bar chart showing the frequencies of $CX3CR1^+CD27^-$ NK cells in EAC patient blood ($n = 7$), omentum ($n = 7$), and tumor ($n = 6$). (D) Right, Representative dot plot showing $CX3CR1^+CD27^-$ NK cells (cytotoxic population) in EAC patient blood. (**E**) Left, Bar chart showing frequencies of $CX3CR1^+$L-$selectin^+$ NK cells in EAC patient blood ($n = 6$), omentum ($n = 4$), and tumor ($n = 9$). (E) Right, Representative dot plot showing population of effector $CX3CR1^+$L-$selectin^+$ NK cells in EAC patient blood. Mean + SEM. $^*p < 0.05$, $^{**}p < 0.01$, $^{****}p < 0.0001$ by one-way ANOVA.

(Fig. 7A). Similarly, whereas there were significant levels of NK cell–mediated killing of K562 cells, there were no significant differences in the level of K562 cell death between untreated NK cells or fractalkine-treated NK cells ($n = 5$) (Fig. 7B).

Frequencies of circulating $CX3CR1^+$ NK cells are highest following CRT in EAC patients

To elucidate the optimal time point at which to target $CX3CR1^+$ NK cell migration to omentum with systemic CX3CR1 antagonism, we quantified total and $CX3CR1^+$ NK cell frequencies in the blood and tumor of a total of 12 treatment-naive EAC patients and a total of 36 EAC patients at a time point following neoadjuvant CRT.

Our data revealed significantly higher frequencies of circulating NK cells in EAC patients following neoadjuvant CRT: treatment naive versus post-CRT (1.2 versus 7.89%, $p = 0.0001$) (Fig. 8A). Interestingly, no significant differences were observed in the frequencies of intratumoral NK cells between treatment-naive EAC patients and those who received CRT (Fig. 8A). In parallel with total frequencies of NK cells, frequencies of circulating $CX3CR1^+$ NK cells were significantly higher in EAC patients following CRT; treatment naive versus post-CRT (44.5 versus 69.9%, $p = 0.0085$) (Fig. 8B).

Discussion

Novel immunotherapeutic approaches are urgently required to improve the dismal outcomes for EAC patients (4–8). We have previously reported the active recruitment of cytotoxic immune cells to the chemotactic cues of the omentum in EAC, and we propose that such misguided immune cell migration compromises antitumor immunity and poses a significant challenge for immunotherapeutic efficacy in these patients (11, 12). Furthermore, we have reported that NK cell phenotype, function, and viability is altered by soluble mediators in the microenvironment of EAC omentum, potentially reducing their ability to elicit effective antitumor immunity (12). To this end, we propose that harnessing NK cell responses and migratory pathways in EAC provides a means of augmenting antitumor immunity. This in vitro study used CX3CR1 antagonism to examine whether the CX3CR1 ligand fractalkine is a key NK cell

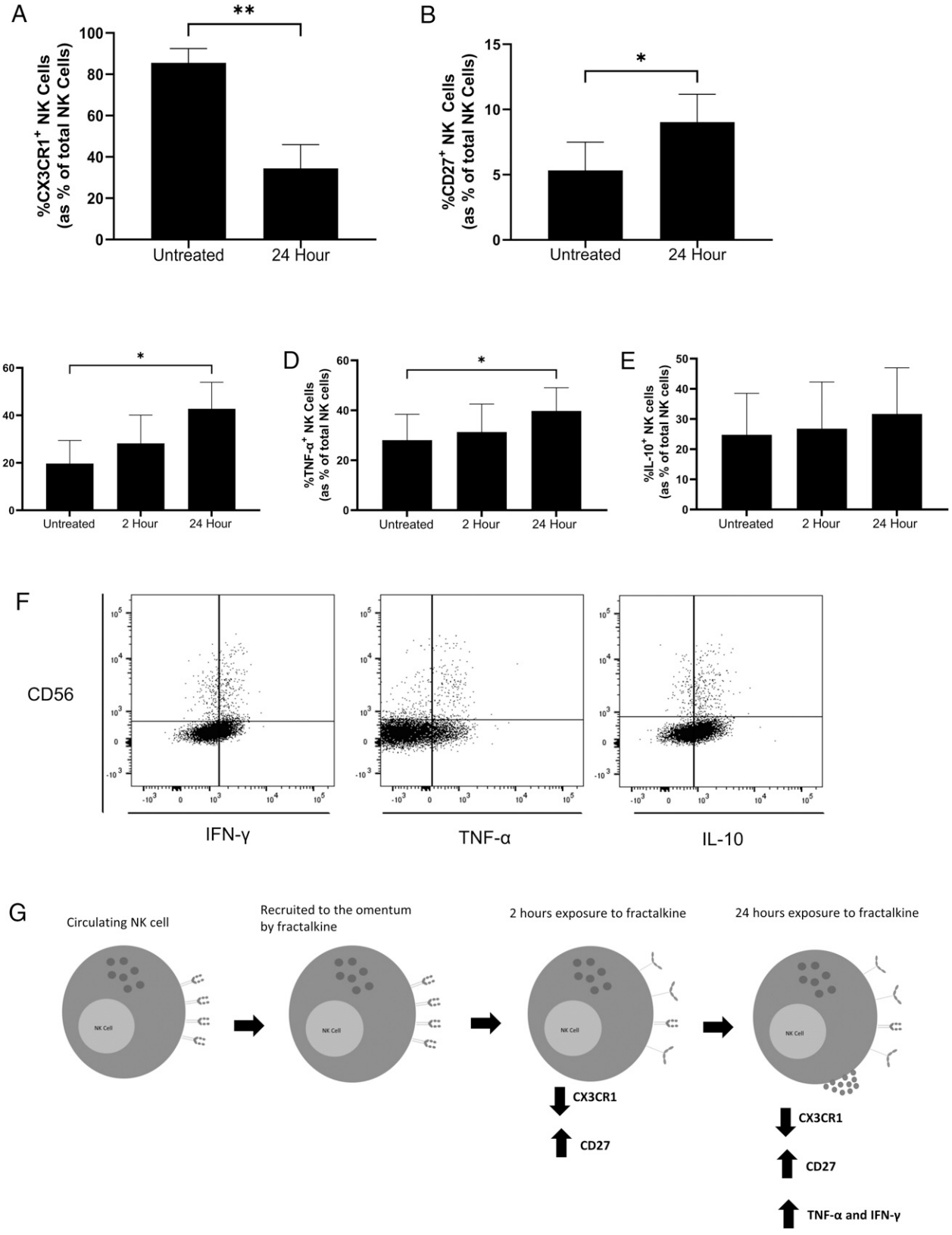

FIGURE 6. Fractalkine-mediated enhancement of proinflammatory cytokine production by NK cells. (**A**) Bar chart showing the frequency of CX3CR1$^+$ NK cells following no treatment (Untreated) or treatment with 30 ng/ml recombinant fractalkine for 24 h ($n = 5$). (**B**) Bar chart showing the frequency of CD27$^+$ NK cells following no treatment or treatment with 30 ng/ml recombinant fractalkine for 24 h ($n = 3$). Left, Bar chart showing the frequencies of (**C**) IFN-γ$^+$, (**D**) TNF-α$^+$, and (**E**) IL-10$^+$ NK cells as a percentage of total NK cells following no treatment or treatment with 30 ng/ml recombinant fractalkine for 2 or 24 h ($n = 6$). (**F**) Representative dot plots showing peripheral blood–derived (left) IFN-γ$^+$, (middle) TNF-α$^+$, and (right) IL-10$^+$ NK cells previously gated on total lymphocytes. (**G**) Schematic showing the fate of NK cells in EAC. NK cells are recruited to the omentum in EAC by fractalkine. Exposure to fractalkine for 2 h significantly decreases the frequency of CX3CR1$^+$ NK cells and significantly increases the frequency of CD27$^+$ NK cells. Following exposure to fractalkine for 24 h, there are significantly lower frequencies of CX3CR1$^+$ and significantly higher frequencies of CD27$^+$, IFN-γ$^+$, and TNF-α$^+$ NK cells. Mean + SEM. *$p < 0.05$, **$p < 0.01$ by paired t test or one-way ANOVA.

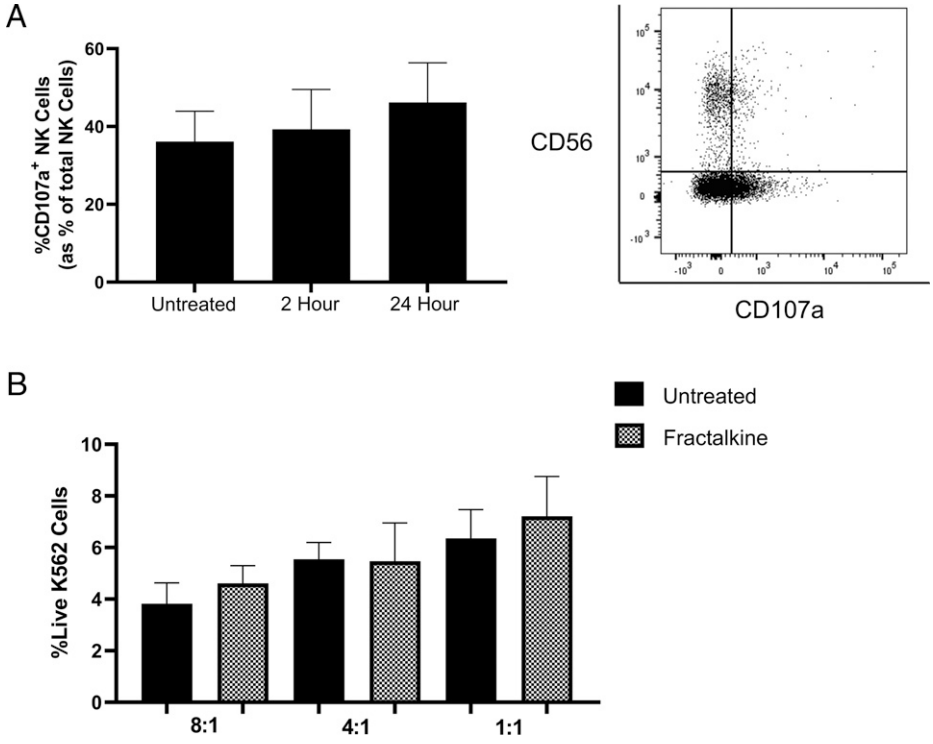

FIGURE 7. Fractalkine elicits no significant effects on NK cell degranulation or cytotoxicity. (**A**) Left, Bar chart showing the frequency of $CD107a^+$ NK cells following no treatment (Untreated) or treatment with 30 ng/ml recombinant fractalkine for 2 or 24 h ($n = 6$). Right, Representative dot plots showing peripheral blood–derived $CD107a^+$ NK cells previously gated on total lymphocytes. (**B**) Bar chart showing the frequency of live K562 cells following coincubation with NK cells left untreated (black) or pretreated with 30 ng/ml fractalkine for 24 h (patterned) at effector target ratios of 8:1, 4:1, and 1:1 ($n = 5$). By one-way ANOVA. Mean + SEM.

chemoattract in EAC patient–derived omental tissue and tumor tissue. In doing so, we aimed to identify a potential target for reducing NK cell chemotaxis to soluble factors in EAC patient–derived omentum.

It is well established that NK cell infiltration of solid tumors is associated with a better prognosis, and as such, therapeutically boosting NK cell migration to EAC tumors is a desirable concept (13, 14). Our data demonstrate that NK cell frequencies are lower in EAC tumor tissue compared with the other compartments examined and moreover that such frequencies decrease as visceral obesity increases. Because lower intratumoral frequencies of NK cells have been associated with poorer prognosis in esophageal and gastric cancer, we propose that modest NK cell tumor infiltrates in the most viscerally obese EAC patients are indicative of less-effective NK cell–mediated antitumor immune responses in this cohort (13, 14). The diminished numbers of NK cells in EAC omentum are in line with our group's previous findings, which demonstrated that soluble factors within the omental microenvironment induce NK cell apoptosis and reduce the frequencies of cytotoxicity receptor–bearing populations of $NKp46^+$ and $NKp30^+$ NK cells, thus contributing to the lower frequency of $NKp46^+$ NK cells observed in EAC omentum (12). In the current study, our data provide further supporting evidence by revealing substantially higher levels of apoptosis in NK cells derived from EAC patient omentum, compared with blood. Crucially, our data reveal a negative correlation between VFA and intratumoral NK cell frequencies, suggesting NK cell infiltration of tumor decreases as visceral obesity increases in EAC patients, and we propose that this is due, at least in part, to migration to and apoptosis within the omentum (12). This correlation is not observed with BMI, thus emphasizing the importance of visceral adiposity as a pathological entity compared with overall adiposity and supporting the classification of visceral obesity as most detrimental for human health (31).

A role for the multifunctional inflammatory chemokine fractalkine in macrophage-mediated inflammation in obese adipose tissue and in $CD8^+$ T cell recruitment to and alteration in the omentum in EAC has been established (11, 24, 34, 39). As such, we proposed that fractalkine may also govern the erroneous migration of NK

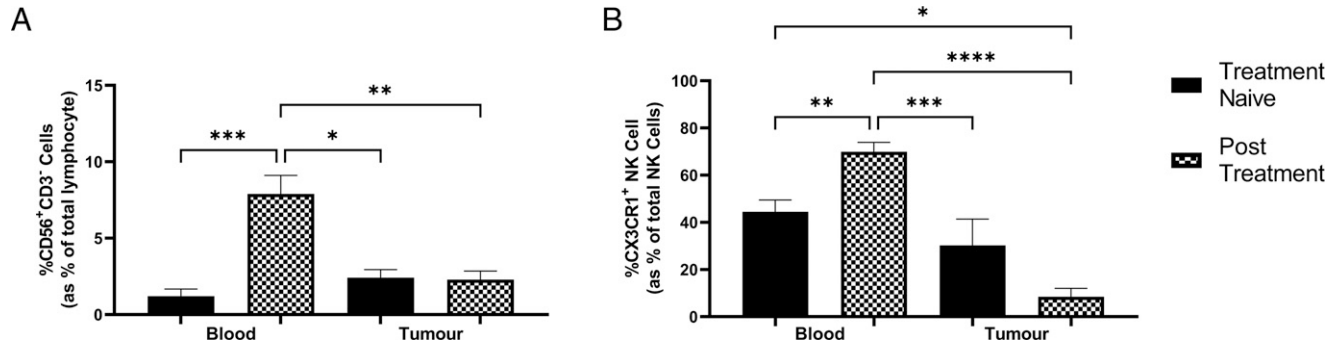

FIGURE 8. Frequencies of circulating $CX3CR1^+$ NK cells are significantly higher following neoadjuvant CRT in EAC patients. (**A**) Bar chart showing percentages of total NK cells in treatment-naive EAC patient (black) and post-CRT EAC patient (pattern) blood (treatment naive, $n = 12$; post-CRT, $n = 21$) and tumor (treatment naive, $n = 7$; post-CRT, $n = 10$). (**B**) Bar chart showing $CX3CR1^+$ NK cells in treatment-naive EAC patient (black) and post-CRT EAC patient (pattern) blood (treatment naive, $n = 12$; post-CRT, $n = 36$) and tumor (treatment naive, $n = 7$; post-CRT, $n = 6$). Mean + SEM. $*p < 0.05$, $**p < 0.01$, $***p < 0.001$, $****p < 0.0001$ by one-way ANOVA.

cells to the omentum in EAC. To our knowledge, this is the first report that CX3CR1 antagonism can significantly reduce the recruitment of NK cells to the chemotactic signals of EAC omentum, but, importantly, not tumor. This was somewhat expected, as we have previously shown that the CX3CR1 ligand is one of the most abundant chemokines in EAC omentum, but not in the tumor (11, 27).

Expression of CX3CR1 on noncancer NK cells is well documented (30, 40, 41). Our data reveal that NK cells in the circulation of EAC patients express abundant levels of CX3CR1. This indicates high susceptibility to systemic administration of CX3CR1 antagonist, which may facilitate the therapeutic maintenance of NK cell numbers in EAC by preventing their migration to and demise within the omentum, ultimately increasing their availability to potentially migrate to alternative signals in EAC tumor, namely MIP-1α, MIP-3α, and RANTES (27). These data are in line with our group's previous report that demonstrated that the highest frequencies of $CX3CR1^+$ cytotoxic $CD8^+$ T cells were present in EAC patient blood (11). CX3CR1 antagonism may prevent the loss of multiple cytotoxic lymphocyte subsets in the visceral fat of EAC patients and in other obesity-associated cancers in which immunotherapy efficacy is compromised (2, 11, 12, 25). CX3CR1 antagonism also holds therapeutic potential for use in combination with other immunotherapies to prevent NK cell recruitment to the omentum and, in doing so, maximize their availability to potentially infiltrate the tumor in obese cancer patients. For instance, adoptive transfer of immune cells has had limited success for solid malignancies, and the efficacy of such treatments could be enhanced using chemokine-targeted therapies to improve tumor homing (42). With regard to patient-derived NK cell therapies, it has been established that the cytotoxic $CD56^{dim}$ NK cell subset expresses the highest levels of CX3CR1, making prevention of their accumulation and demise in the omentum of paramount importance for effective antitumor immunity in obese cancer patients (40, 41). Additionally, the expression of CX3CR1 has been confirmed on the Food and Drug Administration–approved NK cell line NK-92, indicating their susceptibility to CX3CR1 antagonism and suitability as a potential combination immunotherapy for EAC and other obesity-associated malignancies (43, 44).

We have previously reported that high levels of fractalkine in the omentum of EAC patients can induce endocytosis of CX3CR1 by $CD8^+$ T cells, leading to lower frequencies of omental $CD8^+$ T cells expressing the receptor on their surface, and that such internalization is exclusive to T cells expressing high levels of the receptor, whereas $CD4^+$ T cells were not susceptible to the effects of fractalkine (11). In this study, we report significant decreases in CX3CR1 expression on NK cells following exposure to fractalkine, strongly supporting the hypothesis that fractalkine contributes to the lower surface expression of CX3CR1 on omental NK cells in EAC and reaffirming that fractalkine recruits and regulates cells that are high expressers of CX3CR1 (11). Fractalkine-mediated reduction of CX3CR1 surface expression by these key antitumor immune cells is further indication of its broader effects on cytotoxic lymphocytes in cancer (11).

CD27 has emerged as an alternative marker of NK cell maturation and function (28, 35). $CD27^+$ NK cells have distinct functional profiles akin to the $CD56^{bright}$ subset, producing high levels of IFN-γ and TNF-α (28, 35). Like T cells, a loss of CD27 expression on NK cells marks the differentiation toward an effector cell phenotype akin to the $CD56^{dim}$ subset that possesses potent cytotoxic effector functions and contains high levels of granzyme B and perforin (28, 35, 45). Previous reports have suggested that the majority of circulating NK cells are $CD27^-$, with $CD27^+$ NK cells enriched within the secondary lymphoid organs, which include omentum (28, 35, 46). In congruence with these reports, we have identified an abundance of the cytokine-producing $CD27^+$ NK cell subset within the omentum of EAC patients, compared with the circulation and tumor. These data are also in line with our group's previous reports of a shift to a less-cytotoxic NK cell profile within the omental microenvironment (12). Furthermore, our data demonstrated that fractalkine treatment significantly increased the frequencies of $CD27^+$ NK cells, strongly suggesting that this chemokine is contributing to the $CX3CR1^-CD27^+$ phenotype within EAC omentum. Interestingly, this fractalkine-induced increase in CD27 was not accompanied by any alterations in NK cell cytotoxicity.

To ascertain whether the fractalkine-mediated alterations in CD27 expression mirrored alterations in the cytokine-producing capabilities of NK cells, we examined the production of IFN-γ, TNF-α, and IL-10 following exposure to fractalkine. Interestingly, fractalkine significantly increased the production of proinflammatory cytokines by NK cells. These data are in line with previous reports by our group that described an abundance of IFN-γ– and TNF-α–producing NK cells within the EAC omentum and identify fractalkine as a key mediator in shaping the functional capacities of NK cells within the omentum (12). In a murine model of obesity, high-fat diet increases IFN-γ production by NK cells and mediates proinflammatory macrophage accumulation within the VAT (47). This suggests fractalkine may be contributing to the abundance of IFN-γ–producing cells and thus the chronic inflammation characteristic of obesity within the VAT.

A previous study reporting expression analysis of CD27 and CX3CR1 on NK cells shows a sequential decrease in CD27 expression as NK cells mature, suggesting the most mature, cytotoxic NK cells are $CX3CR1^+CD27^-$ (28, 30, 35). Our data demonstrate that such $CX3CR1^+CD27^-$ NK cells are most prevalent within the circulation of EAC patients but are not infiltrating the EAC tumor in the same abundance. In fact, our data indicate that these cells are homing to the fractalkine-rich omentum via the fractalkine/CX3CR1 pathway. Whereas our previous studies demonstrate that many NK cells undergo apoptosis in the omental microenvironment, the data presented in this study strongly indicate that the surviving fraction are converted to a $CX3CR1^+CD27^-$ cytokine-producing NK cell population and that fractalkine is a mediator of this conversion. We propose that preventing recruitment of such $CX3CR1^+CD27^-$ NK cells to omentum via CX3CR1 antagonism is a promising approach to prevent NK cell loss in EAC omentum and increase their availability to migrate toward alternative chemokines in EAC tumor and ultimately enhance NK cell–mediated antitumor immunity (27).

L-$selectin^+$ NK cells have been reported to represent a polyfunctional NK cell subset that possesses full effector functions and an enhanced ability to proliferate (37). A central role for L-selectin in the recruitment of NK cells to both tumor and lymph node and in identifying NK cells with potent effector functions has also been established, suggesting that the migration of L-$selectin^+$ NK cells to tumor would be advantageous (36–38). In this study, we have identified that L-$selectin^+$ NK cells are significantly less abundant in EAC tumor, compared with blood. Because we have identified that a large proportion of these cells coexpress CX3CR1, we propose that the previously described L-$selectin^+CX3CR1^+$ effector population in EAC blood may be amenable to CX3CR1 antagonism, thus providing more compelling evidence to use this strategy to prevent migration of potent effector NK cells to omentum and provide an opportunity for them to home to the chemotactic cues of EAC tumor (27, 30).

For the successful use of novel immunotherapies, it is crucial to identify the optimal timing for administration of these immunotherapies in combination with first-line treatments such as CRT. To effectively target patient-derived NK cells with systemic CX3CR1 antagonism, the treatment would ideally be administered when

frequencies of circulating total and CX3CR1$^+$ NK cells are highest. In this article, we report the optimal timing for combining CX3CR1 antagonism with first-line treatments in EAC patients is following neoadjuvant CRT. Such a sequence of treatments would target NK cell migration when circulating numbers of total and CX3CR1$^+$ NK cells are highest and when the potential is greatest for reducing CX3CR1$^+$ NK cell migration to omentum and freeing them to migrate to alternative signals in tumor.

To our knowledge, this study has uncovered new biological functions of the proinflammatory adipochemokine fractalkine, identifying it as a regulator of NK cell migration, phenotype, and cytokine production in EAC. Our data provide crucial insights into the fate of NK cells in obesity-associated cancer and identify CX3CR1 antagonism as a potential strategy for preventing their erroneous recruitment to omentum to therapeutically limit immune dysfunction in viscerally obese EAC patients.

Acknowledgments

We thank the patients and staff at the Oesophageal and Gastric Centre at St. James's Hospital for participation in this study.

Disclosures

The authors have no financial conflicts of interest.

References

1. World Health Organization. 2020. Obesity and overweight. Available at: https://www.who.int/news-room/fact-sheets/detail/obesity-and-overweight. Accessed: May 5, 2020.
2. Lauby-Secretan, B., C. Scoccianti, D. Loomis, Y. Grosse, F. Bianchini, and K. Straif; International Agency for Research on Cancer Handbook Working Group. 2016. Body fatness and cancer–viewpoint of the IARC working group. *N. Engl. J. Med.* 375: 794–798.
3. Hoyo, C., M. B. Cook, F. Kamangar, N. D. Freedman, D. C. Whiteman, L. Bernstein, L. M. Brown, H. A. Risch, W. Ye, L. Sharp, et al. 2012. Body mass index in relation to oesophageal and oesophagogastric junction adenocarcinomas: a pooled analysis from the International BEACON Consortium. *Int. J. Epidemiol.* 41: 1706–1718.
4. Siegel, R. L., K. D. Miller, and A. Jemal. 2020. Cancer statistics, 2020. *CA Cancer J. Clin.* 70: 7–30.
5. van Hagen, P., M. C. C. M. Hulshof, J. J. B. van Lanschot, E. W. Steyerberg, M. I. van Berge Henegouwen, B. P. L. Wijnhoven, D. J. Richel, G. A. P. Nieuwenhuijzen, G. A. P. Hospers, J. J. Bonenkamp, et al.; CROSS Group. 2012. Preoperative chemoradiotherapy for esophageal or junctional cancer. *N. Engl. J. Med.* 366: 2074–2084.
6. American Society of Clinical Oncology. 2020. Stomach cancer survival rates. Available at: https://www.cancer.org/cancer/stomach-cancer/detection-diagnosis-staging/survival-rates.html. Accessed: May 5, 2020.
7. Ajani, J. A., P. F. Mansfield, N. Janjan, J. Morris, P. W. Pisters, P. M. Lynch, B. Feig, R. Myerson, R. Nivers, D. S. Cohen, and L. L. Gunderson. 2004. Multi-institutional trial of preoperative chemoradiotherapy in patients with potentially resectable gastric carcinoma. *J. Clin. Oncol.* 22: 2774–2780.
8. Ajani, J. A., P. F. Mansfield, C. H. Crane, T. T. Wu, S. Lunagomez, P. M. Lynch, N. Janjan, B. Feig, J. Faust, J. C. Yao, et al. 2005. Paclitaxel-based chemoradiotherapy in localized gastric carcinoma: degree of pathologic response and not clinical parameters dictated patient outcome. *J. Clin. Oncol.* 23: 1237–1244.
9. Vivier, E., E. Tomasello, M. Baratin, T. Walzer, and S. Ugolini. 2008. Functions of natural killer cells. *Nat. Immunol.* 9: 503–510.
10. Waldhauer, I., and A. Steinle. 2008. NK cells and cancer immunosurveillance. *Oncogene* 27: 5932–5943.
11. Conroy, M. J., S. G. Maher, A. M. Melo, S. L. Doyle, E. Foley, J. V. Reynolds, A. Long, and J. Lysaght. 2018. Identifying a novel role for fractalkine (CX3CL1) in memory CD8+ T cell accumulation in the omentum of obesity-associated cancer patients. *Front. Immunol.* 9: 1867.
12. Conroy, M. J., V. Fitzgerald, S. L. Doyle, S. Channon, Z. Useckaite, N. Gilmartin, C. O'Farrelly, N. Ravi, J. V. Reynolds, and J. Lysaght. 2016. The microenvironment of visceral adipose tissue and liver alter natural killer cell viability and function. *J. Leukoc. Biol.* 100: 1435–1442.
13. Xu, B., L. Chen, J. Li, X. Zheng, L. Shi, C. Wu, and J. Jiang. 2016. Prognostic value of tumor infiltrating NK cells and macrophages in stage II+III esophageal cancer patients. *Oncotarget* 7: 74904–74916.
14. Ishigami, S., S. Natsugoe, K. Tokuda, A. Nakajo, X. Che, H. Iwashige, K. Aridome, S. Hokita, and T. Aikou. 2000. Prognostic value of intratumoral natural killer cells in gastric carcinoma. *Cancer* 88: 577–583.
15. Lynch, L. A., J. M. O'Connell, A. K. Kwasnik, T. J. Cawood, C. O'Farrelly, and D. B. O'Shea. 2009. Are natural killer cells protecting the metabolically healthy obese patient? *Obesity (Silver Spring)* 17: 601–605.
16. Theurich, S., E. Tsaousidou, R. Hanssen, A. M. Lempradl, J. Mauer, K. Timper, K. Schilbach, K. Folz-Donahue, C. Heilinger, V. Sexl, et al. 2017. IL-6/Stat3-dependent induction of a distinct, obesity-associated NK cell subpopulation deteriorates energy and glucose homeostasis. *Cell Metab.* 26: 171–184.e6.
17. Viel, S., L. Besson, E. Charrier, A. Marçais, E. Disse, J. Bienvenu, T. Walzer, and C. Dumontet. 2017. Alteration of natural killer cell phenotype and function in obese individuals. *Clin. Immunol.* 177: 12–17.
18. Michelet, X., L. Dyck, A. Hogan, R. M. Loftus, D. Duquette, K. Wei, S. Beyaz, A. Tavakkoli, C. Foley, R. Donnelly, et al. 2018. Metabolic reprogramming of natural killer cells in obesity limits antitumor responses. *Nat. Immunol.* 19: 1330–1340.
19. Bähr, I., V. Goritz, H. Doberstein, G. G. R. Hiller, P. Rosenstock, J. Jahn, O. Pörtner, T. Berreis, T. Mueller, J. Spielmann, and H. Kielstein. 2017. Diet-induced obesity is associated with an impaired NK cell function and an increased colon cancer incidence. *J. Nutr. Metab.* 2017: 4297025.
20. Laue, T., C. D. Wrann, B. Hoffmann-Castendiek, D. Pietsch, L. Hübner, and H. Kielstein. 2015. Altered NK cell function in obese healthy humans. *BMC Obes.* 2: 1.
21. Spielmann, J., J. Hanke, D. Knauf, S. Ben-Eliyahu, R. Jacobs, G. I. Stangl, I. Bähr, and H. Kielstein. 2017. Significantly enhanced lung metastasis and reduced organ NK cell functions in diet-induced obese rats. *BMC Obes.* 4: 24.
22. Charo, I. F., and R. M. Ransohoff. 2006. The many roles of chemokines and chemokine receptors in inflammation. *N. Engl. J. Med.* 354: 610–621.
23. Wensveen, F. M., S. Valentić, M. Šestan, T. Turk Wensveen, and B. Polić. 2015. The "Big Bang" in obese fat: events initiating obesity-induced adipose tissue inflammation. *Eur. J. Immunol.* 45: 2446–2456.
24. Shah, R., C. C. Hinkle, J. F. Ferguson, N. N. Mehta, M. Li, L. Qu, Y. Lu, M. E. Putt, R. S. Ahima, and M. P. Reilly. 2011. Fractalkine is a novel human adipochemokine associated with type 2 diabetes. *Diabetes* 60: 1512–1518.
25. Conroy, M. J., K. C. Galvin, M. E. Kavanagh, A. M. Mongan, S. L. Doyle, N. Gilmartin, C. O'Farrelly, J. V. Reynolds, and J. Lysaght. 2016. CCR1 antagonism attenuates T cell trafficking to omentum and liver in obesity-associated cancer. *Immunol. Cell Biol.* 94: 531–537.
26. Conroy, M. J., K. C. Galvin, S. L. Doyle, M. E. Kavanagh, A. M. Mongan, A. Cannon, G. Y. Moore, J. V. Reynolds, and J. Lysaght. 2016. Parallel profiles of inflammatory and effector memory T cells in visceral fat and liver of obesity-associated cancer patients. *Inflammation* 39: 1729–1736.
27. Kavanagh, M. E., M. J. Conroy, N. E. Clarke, N. T. Gilmartin, R. Feighery, F. MacCarthy, D. O'Toole, N. Ravi, J. V. Reynolds, J. O' Sullivan, and J. Lysaght. 2019. Altered T cell migratory capacity in the progression from Barrett oesophagus to oesophageal adenocarcinoma. *Cancer Microenviron.* 12: 57–66.
28. Vossen, M. T. M., M. Matmati, K. M. L. Hertoghs, P. A. Baars, M.-R. Gent, G. Leclercq, J. Hamann, T. W. Kuijpers, and R. A. W. van Lier. 2008. CD27 defines phenotypically and functionally different human NK cell subsets. *J. Immunol.* 180: 3739–3745.
29. Hayakawa, Y., and M. J. Smyth. 2006. CD27 dissects mature NK cells into two subsets with distinct responsiveness and migratory capacity. *J. Immunol.* 176: 1517–1524.
30. Hamann, I., N. Unterwalder, A. E. Cardona, C. Meisel, F. Zipp, R. M. Ransohoff, and C. Infante-Duarte. 2011. Analyses of phenotypic and functional characteristics of CX3CR1-expressing natural killer cells. *Immunology* 133: 62–73.
31. Doyle, S. L., A. M. Bennett, C. L. Donohoe, A. M. Mongan, J. M. Howard, F. E. Lithander, G. P. Pidgeon, J. V. Reynolds, and J. Lysaght. 2013. Establishing computed tomography-defined visceral fat area thresholds for use in obesity-related cancer research. *Nutr. Res.* 33: 171–179.
32. Lysaght, J., E. H. Allott, C. L. Donohoe, J. M. Howard, G. P. Pidgeon, and J. V. Reynolds. 2011. T lymphocyte activation in visceral adipose tissue of patients with oesophageal adenocarcinoma. *Br. J. Surg.* 98: 964–974.
33. Melo, A. M., A. M. O'Brien, J. J. Phelan, S. A. Kennedy, N. A. W. Wood, N. Veerapen, G. S. Besra, N. E. Clarke, E. K. Foley, A. Ravi, et al. 2019. Mucosal-associated invariant T cells display diminished effector capacity in oesophageal adenocarcinoma. *Front. Immunol.* 10: 1580.
34. Conroy, M. J., and J. Lysaght. 2020. CX3CL1 signaling in the tumor microenvironment. In *Tumor Microenvironment. Advances in Experimental Medicine and Biology*, Vol. 1231. A. Birbrair, ed. Springer, Cham, Switzerland. p. 1–12.
35. Silva, A., D. M. Andrews, A. G. Brooks, M. J. Smyth, and Y. Hayakawa. 2008. Application of CD27 as a marker for distinguishing human NK cell subsets. *Int. Immunol.* 20: 625–630.
36. Sobolev, O., P. Stern, A. Lacy-Hulbert, and R. O. Hynes. 2009. Natural killer cells require selectins for suppression of subcutaneous tumors. *Cancer Res.* 69: 2531–2539.
37. Juelke, K., M. Killig, M. Luetke-Eversloh, E. Parente, J. Gruen, B. Morandi, G. Ferlazzo, A. Thiel, I. Schmitt-Knosalla, and C. Romagnani. 2010. CD62L expression identifies a unique subset of polyfunctional CD56dim NK cells. *Blood* 116: 1299–1307.
38. Chen, S., H. Kawashima, J. B. Lowe, L. L. Lanier, and M. Fukuda. 2005. Suppression of tumor formation in lymph nodes by L-selectin-mediated natural killer cell recruitment. *J. Exp. Med.* 202: 1679–1689.
39. D'Haese, J. G., I. E. Demir, H. Friess, and G. O. Ceyhan. 2010. Fractalkine/CX3CR1: why a single chemokine-receptor duo bears a major and unique therapeutic potential. *Expert Opin. Ther. Targets* 14: 207–219.

40. Stabile, H., P. Nisti, S. Morrone, D. Pagliara, A. Bertaina, F. Locatelli, A. Santoni, and A. Gismondi. 2015. Multifunctional human CD56 low CD16 low natural killer cells are the prominent subset in bone marrow of both healthy pediatric donors and leukemic patients. *Haematologica* 100: 489–498.
41. Campbell, J. J., S. Qin, D. Unutmaz, D. Soler, K. E. Murphy, M. R. Hodge, L. Wu, and E. C. Butcher. 2001. Unique subpopulations of CD56+ NK and NK-T peripheral blood lymphocytes identified by chemokine receptor expression repertoire. *J. Immunol.* 166: 6477–6482.
42. Nayyar, G., Y. Chu, and M. S. Cairo. 2019. Overcoming resistance to natural killer cell based immunotherapies for solid tumors. *Front. Oncol.* 9: 51.
43. Klingemann, H., L. Boissel, and F. Toneguzzo. 2016. Natural killer cells for immunotherapy - advantages of the NK-92 cell line over blood NK cells. *Front. Immunol.* 7: 91.
44. Zhang, X., H. Wei, H. Wang, and Z. Tian. 2006. Involvement of interaction between fractalkine and CX3CR1 in cytotoxicity of natural killer cells against tumor cells. *Oncol. Rep.* 15: 485–488.
45. Hamann, D., P. A. Baars, M. H. G. Rep, B. Hooibrink, S. R. Kerkhof-Garde, M. R. Klein, and R. A. W. van Lier. 1997. Phenotypic and functional separation of memory and effector human CD8+ T cells. *J. Exp. Med.* 186: 1407–1418.
46. Meza-Perez, S., and T. D. Randall. 2017. Immunological functions of the omentum. *Trends Immunol.* 38: 526–536.
47. Wensveen, F. M., V. Jelenčić, S. Valentić, M. Šestan, T. T. Wensveen, S. Theurich, A. Glasner, D. Mendrila, D. Štimac, F. T. Wunderlich, et al. 2015. NK cells link obesity-induced adipose stress to inflammation and insulin resistance. *Nat. Immunol.* 16: 376–385.